Synergistic effect of steel fibres and coarse aggregates on impact properties of ultra-high performance fibre reinforced concrete

Cement and Concrete Composites 115 (2021) 103866

Contents lists available at ScienceDirect

Cement and Concrete Composites

journal homepage: http://www.elsevier.com/locate/cemconcomp

Synergistic effect of steel fibres and coarse aggregates on impact properties of ultra-high performance fibre reinforced concrete

P.P. Li [a,b], Y.Y.Y. Cao [b], M.J.C. Sluijsmans [b], H.J.H. Brouwers [b], Qingliang Yu [b,c,*]

[a] School of Civil Engineering and Architecture, Wuhan University of Technology, Wuhan, 430070, PR China
[b] Department of the Built Environment, Eindhoven University of Technology, P.O. Box 513, 5600 MB, Eindhoven, the Netherlands
[c] School of Civil Engineering, Wuhan University, Wuhan, 430072, PR China

ARTICLE INFO

Keywords:
Synergistic effect
Ultra-high performance fibre reinforced concrete
Impact resistance
Flexural property
Steel fibre
Coarse aggregate

ABSTRACT

This study investigates the synergistic effect of steel fibres and coarse aggregates on impact behaviour of ultra-high performance fibre reinforced concrete (UHPFRC). UHPFRC matrices with a low cement content and maximum aggregate sizes of 8 mm and 25 mm are designed by using a particle packing model. Three types of steel fibres (13 mm short straight, 30 mm medium hook-ended and 60 mm long 5D) are studied in terms of the utilization efficiencies. The results show that UHPFRC with coarser aggregates tends to have a lower cement consumption but slightly weaker mechanical strength, and the largest aggregate size is suggested to be no more than 25 mm considering the reduction on flexural toughness and impact resistance. The medium and long fibres contribute to an excellent deflection/strain hardening behaviour instead of short ones. A preferential synergistic effect on impact and flexural properties is observed between the medium fibres and the finer aggregates, while the longer fibres are more compatible to the coarser aggregates. The length of steel fibre is recommended between 2 and 5 times the maximum aggregate size. The flexural strength controls the impact resistance under low-energy impact loadings, and flexural toughness determines it under relatively high-energy (beyond energy threshold) impact loadings.

1. Introduction

Ultra-high performance fibre reinforced concrete (UHPFRC) possesses superior properties [1–5] due to its special mix design methods and utilized raw ingredients, usually incorporating high steel fibre content and large amount of cement [6–8]. Its excellent mechanical strength and energy absorption capacity contribute to broad applications in civil, protective and military engineering under both static and impact loadings [4,9,10].

The traditional UHPFRC consumes a large amount of cement without applying coarse aggregate to increase homogeneity and eliminate inherent weakness, such as defect of interfacial transition zone (ITZ) between matrix and coarse aggregate, stress concentration in point-to-point contact of aggregates [3,11,12]. It results in a cement consumption three times greater than normal strength concrete, consequently causing environmental and economical burdens [13,14]. To reduce the cost and broaden its application, normal natural sand has been successfully used to replace the expensive quartz sand [15]. Nowadays, some researchers attempt to introduce coarse aggregates into UHPFRC systems in order to further reduce the cost and extend its engineering application [16–21]. Our previous studies have proven that high strength coarse aggregates, e.g. basalt aggregates, can be successfully introduced into a UHPFRC system, which greatly reduce the cement amount and cost [5,16]. Furthermore, concrete incorporating coarse aggregates can also enhance volume stability [17], improve projectile impact resistance [18], achieve better workability, sometimes even a higher strength [19,20], and increase the transition point of stress-strain curves under confined conditions [21]. However, none of these studies have systematically researched the size influence of coarse aggregates in UHPFRC systems. In this study, coarse aggregates with the maximum size (D_{max}) from 8 mm to 25 mm are utilized to investigate their influence on both flexural and impact properties.

Steel fibres are considerably efficient to improve the mechanical and impact resistance of UHPFRC, especially for enhancing the stress transfer capability beyond elastic state and then strengthening the toughness and energy absorption capacity [22,23]. Nevertheless, high strength steel fibres are much more expensive compared to the other solid ingredients in UHPFRC. Furthermore, the reinforcement degree is

* Corresponding author. Department of the Built Environment, Eindhoven University of Technology, P.O. Box 513, 5600 MB, Eindhoven, the Netherlands.
E-mail address: q.yu@bwk.tue.nl (Q. Yu).

https://doi.org/10.1016/j.cemconcomp.2020.103866
Received 27 September 2019; Received in revised form 22 July 2020; Accepted 2 November 2020
Available online 7 November 2020

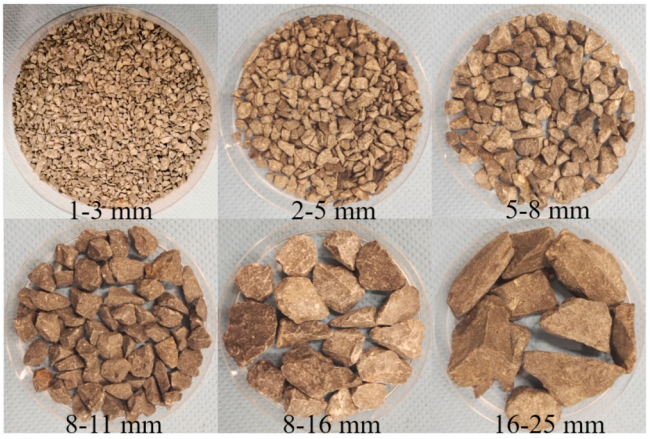

Fig. 1. The basalt aggregates.

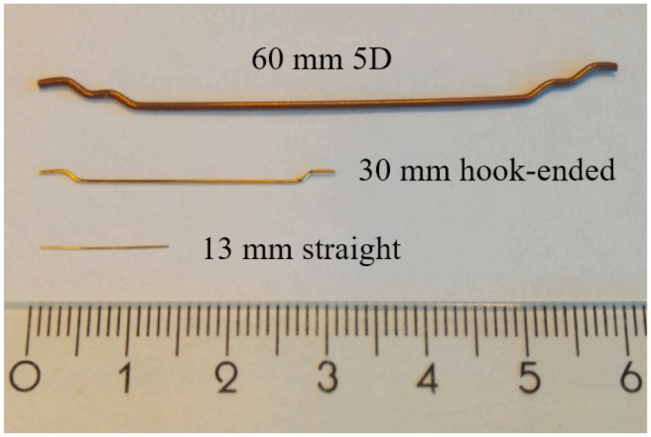

Fig. 2. The steel fibres.

significantly influenced by fibre characteristics, such as fibre content [24,25], shape [26,27], orientation [11,28] and hybridization [29]. Therefore, the appropriate type and content of steel fibre should be carefully researched to achieve an optimal utilization efficiency. As previously reported [22,30,31], two methods are well-known to enhance the flexural properties and energy absorption ability, namely utilizing hook-ended or twisted steel fibres, and enlarging the length of steel fibres. However, relevant research in UHPFRC incorporating coarse aggregates are very scarce.

The reinforcement of steel fibres is dependent on not only the fibre characteristics but also matrix properties (e.g. particle size, strength, shrinkage) and fibre-to-matrix bond. The presence of coarse aggregates in concrete has considerable effects on fibre distribution, dispersion and interfacial bonds, consequently influencing the fibre utilization efficiency [32]. Coarser aggregates tend to need longer steel fibres to overlay and provide enough bridging effect between them on static properties of normal fibre reinforced concrete [33]. But, too long fibres conversely cause mixing and casting problems, as well as disturbance in compactness of the granular skeleton [34]. However, how to use appropriate fibres to outbalance those benefits and drawbacks is very important but still not clear, especially for the dynamic properties of UHPFRC incorporating coarse aggregates under impact loadings. It is therefore very important to research the synergistic effect between steel fibres and coarse aggregates in UHPFRC systems for making full use of their potential.

The objective of this paper is to explore the synergistic effect between steel fibres and coarse aggregates on impact properties of UHPFRC. The effect of the D_{max} from 8 mm to 25 mm, steel fibre type (short straight, medium hook-ended and long 5D), and interaction between coarse aggregates and steel fibres are analysed. Furthermore, a correlation between impact resistance and static mechanical properties is established. Based on the results of impact and flexural behaviour, appropriate sizes of coarse aggregates and corresponding suitable lengths of steel fibres are suggested.

2. Experimental program

2.1. Materials

The ingredients of UHPFRC mixtures include Portland cement (PC), limestone powder (LP), micro-silica (mS), normal sand (S), coarse basalt aggregates (BA) with different sizes, steel fibres with different types (SF), superplasticizer (SP) and tap water (W). The physical and chemical properties of powders can be found in our previous studies [16,35]. Fig. 1 shows the utilized six coarse basalt aggregates with different particle size fractions. Three different steel fibres are used, namely 13 mm (short) straight fibre, 30 mm (medium) hook-ended fibre and 60 mm (long) 5D fibre. Table 1 and Fig. 2 present the characteristics and shapes of steel fibres. Fig. 3 shows the particle size distributions (PSD) of powders and aggregates.

2.2. Mix design

Table 2 presents the recipes of UHPFRC matrices, and Table 3 shows the research variables including basalt aggregate sizes and steel fibres type used in UHPFRC. The limestone powder and micro-silica contents are 20% and 5% of total powders' by mass, following our previous research [16]. 900 kg/m^3 powder are used in the mixtures incorporating the maximum basalt size of 8 mm. While, the powder content is reduced to 700 kg/m^3 for UHPFRC with coarser basalt aggregates (maximum size of 25 mm), considering the fact that coarse aggregates contribute to less demand of powder in concrete [16,17,36]. The contents of aggregates are calculated based on the Brouwers method [37–39],

$$P(D) = \frac{D^q - D_{min}^q}{D_{max}^q - D_{min}^q} \quad (1)$$

$$RSS = \sum_{i=1}^{n} \left[P_{mix}\left(D_i^{i+1}\right) - P_{target}\left(D_i^{i+1}\right) \right]^2 \rightarrow min \quad (2)$$

where D is the particle size. $P(D)$ is the cumulative fraction of all the particles that are smaller than size D. The key parameter in this model is the distribution modulus q, and a small q value of 0.19 is proposed and

Table 1
Characteristics of steel fibres.

Length, l (mm)	Fibre shape	Diameter, d (mm)	Aspect ratio, l/d	Density (kg/m^3)	Tensile strength (MPa)	Elastic modulus (GPa)	Number of fibres per kg
13	Short straight	0.21	62	7850	2750	200	27000
30	Medium hood-ended	0.38	79	7850	2300	210	3600
60	Long 5D	0.9	65	7850	2300	210	2300

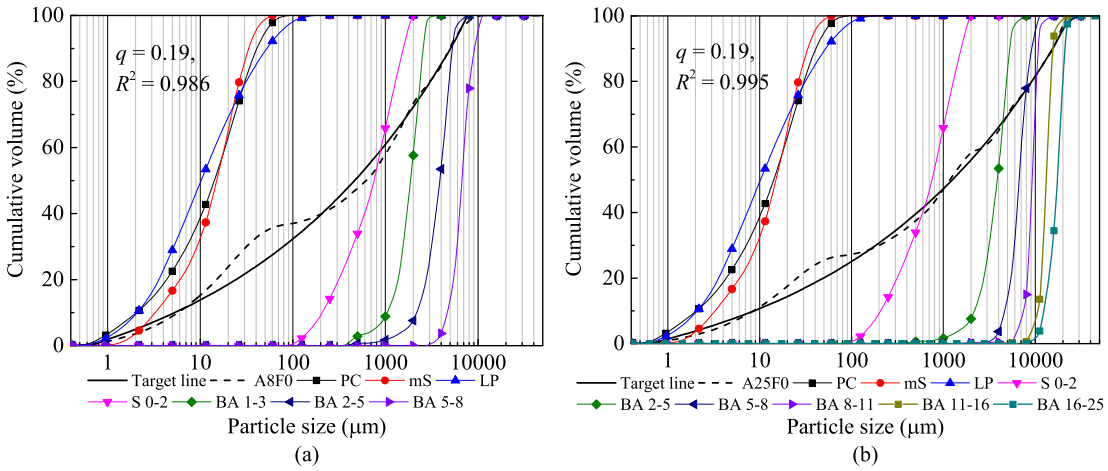

Fig. 3. The PSD of raw materials and UHPFRC matrices.

Table 2
Recipes of designed UHPFRC matrixes (kg/m^3).

Mix No.	Powder	PC	mS	LP	S 0–2	BA 1–3	BA 2–5	BA 5–8	BA 8–11	BA 8–16	BA 16–25	W	SP
A8F0	900	675	45	180	640	198	403	194	0	0	0	174.2	5.8
A25F0	700	525	35	140	667	0	367	173	121	64	365	154.7	4.9

utilized for UHPFRC mixtures with inclusion of coarse aggregates and low powder contents based on our previous research [16]. The quality of fit between the designed and target lines is evaluated by the coefficient of determination,

$$R^2 = 1 - \frac{\sum_{i=1}^{n}\left[P_{mix}\left(D_i^{i+1}\right) - P_{target}\left(D_i^{i+1}\right)\right]^2}{\sum_{i=1}^{n}\left[P_{mix}\left(D_i^{i+1}\right) - \frac{1}{n}\sum_{i=1}^{n}P_{mix}\left(D_i^{i+1}\right)\right]^2} \quad (3)$$

The PSD curves of the designed and target UHPFRC matrices are shown in Fig. 3. The water and superplasticizer amounts are adjusted to achieve self-compacting. The dosages of different steel fibres are fixed at 2% by the volume (vol.) of mixture.

2.3. Testing methods

2.3.1. Compressive and tensile splitting test

The tensile splitting and compressive strengths of concrete samples are tested, three specimens for each mixture, in accordance with EN 12390-6: 2009 [40] and EN 12390-3: 2009 [41], respectively. Fresh concrete is cast into moulds (150 × 150 × 150 mm^3) and demoulded after 1 day. After that, the samples are cured in water (around 20 °C) for another 27 days before testing. The hardboard packing strips in EN 12390-6: 2009 cannot withstand UHPFRC and are replaced by steel ones. The specimens and set-ups are shown in Fig. 4.

2.3.2. Central point flexural test

The central point flexural test for each UHPFRC mixture is conducted by a beam (150 × 150 × 550 mm^3) with the span (l) of 450 mm, in accordance with EN 12390-5: 2009 [42], as shown in Fig. 5(a). Based on the central point flexural tests, the load-deflection curves and corresponding key parameters can be obtained, as illustrated in Fig. 5(b), such as first crack load and deflection, peak load and deflection, and toughness, as well as three stages (elastic stage, deflection/strain hardening stage, deflection/strain softening stage).

2.3.3. Pendulum impact test

A pendulum device is designed to investigate the impact resistance of UHPFRC beams, one specimen for each mixture, which have the same size to those in flexural test mentioned above. The pendulum device has a flexible impact mass (22–40 kg) and height (0–4 m), as shown in Fig. 6. First, UHPFRC beam is hung by steel ropes with a span of 450 mm. Then, the hammer is released from a fixed position and perpendicularly impacted on the central point of UHPFRC beam at the lowest hammer position. Afterwards, both the highest positions of sample and hammer are recorded during the first post-impact swing by a high-speed camera. The impact resistance of UHPFRC is described by the impact number and energy absorption E(J) for each impact is obtained by,

Table 3
Research variables for UHPFRC.

Mix No.	Short straight fibre (13 mm)	Medium hook ended fibre (30 mm)	Long 5D fibre (60 mm)	Max. size of aggregate, D (mm)	L/D_{max}
A8F0				8	0
A8F13	2%				1.625
A8F30		2%			3.75
A8F60			2%		7.5
A25F0				25	0
A25F13	2%				0.52
A25F30		2%			1.2
A25F60			2%		2.4

Note: the values in Mix No. respectively represent the maximum size of aggregate and the length of steel fibre used in the designed UHPFRC, and 0 means plain UHPFRC without steel fibre.

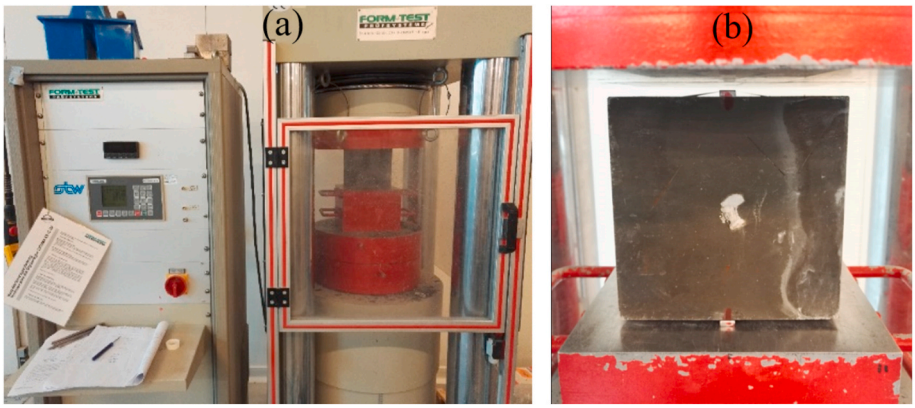

Fig. 4. Specimens and set-ups of (a) compressive and (b) tensile splitting tests.

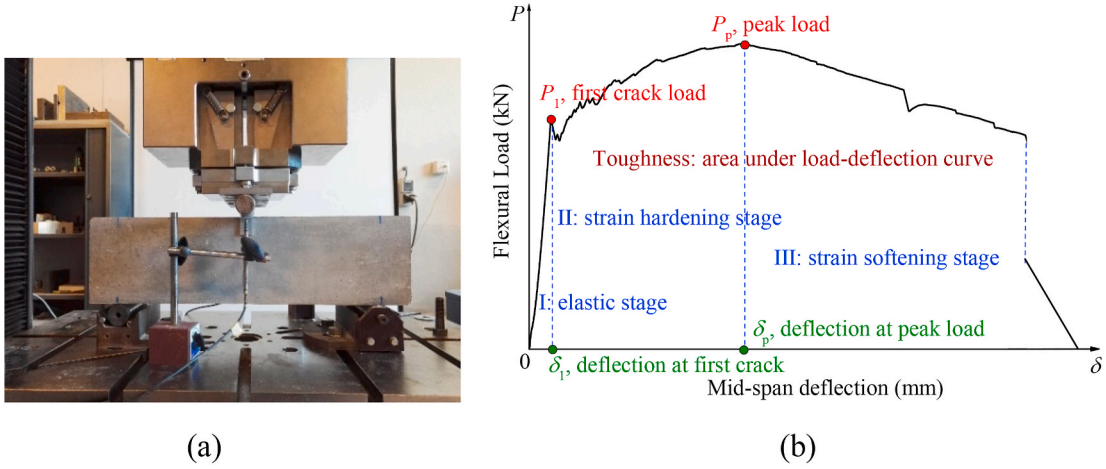

Fig. 5. (a) Flexural test device and (b) key parameters.

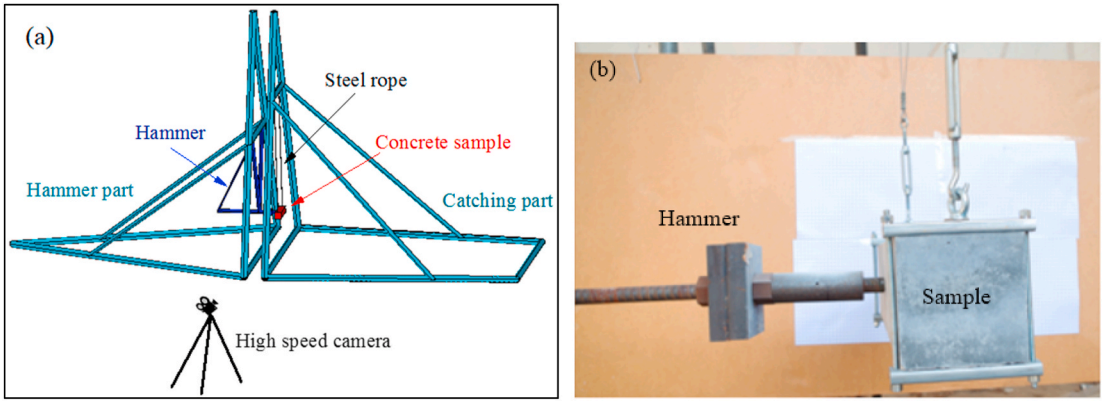

Fig. 6. Pendulum impact device: (a) scheme and (b) impact at the lowest position.

$$E = M_h g(H_h - h_h) - M_s g h_s \quad (4)$$

where M_h(30.3 kg) and H_h(2.35 m) are the mass and initial height of hammer, the specimen mass $M_s$varies for different UHPFRC beams, gravity acceleration $g = 9.8$ m/s^2, the maximum heights of hammer (h_h) and beam (h_s) are measured after impact. To obtain a moderate impact number, the pendulum hammer mass and its initial height in this study are chosen based on preliminary trials, consequently achieving an initial hammer energy of about 698 J. The impact is repeated till the complete failure (fracture) of UHPFRC beam, and the total absorbed energy E_{absorb} can be obtained.

3. Results and discussion

3.1. Static mechanical properties

Fig. 7 presents the compressive strength of the designed UHPFRC after 28 days. With increasing the maximum size of coarse aggregate from 8 mm to 25 mm, the compressive strength of the plain concrete reduces from 137.2 MPa to 124.3 MPa. Although the compressive

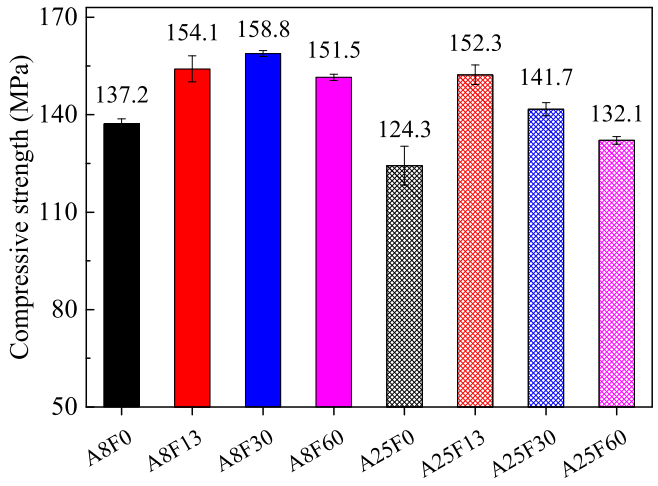

Fig. 7. Compressive strength.

strength has a decrease trend because of the coarse aggregates, the decrease degree is less than 10%, which is in line with our previous result [16]. In addition, the UHPFRC matrix with coarser basalt aggregates tends to have a lower powder demand with even a better quality of fit, namely, powder of 700 kg/m^3 and a R^2 of 0.995 for the mixture A25F0, compared to 900 kg/m^3 and 0.986 for the mixture A8F0. Furthermore, the binder efficiency, defined as 28 days compressive strength normalized by binder amount, can be greatly improved from 0.152 MPa/(kg/m^3) at the mixture A8F0 up to 0.178 MPa/(kg/m^3) at the mixture A25F0. With the inclusion of 2 vol% steel fibres in the matrix (D_{max} = 8 mm), the compressive strength can be enhanced in the range between 10.4% and 15.7%. The 30 mm medium hook-ended steel fibres show the best reinforcement, possessing slightly larger compressive strength than the 13 mm short straight fibres, followed by the 60 mm long 5D fibres. The reinforcement ratio in UHPFRC with coarser aggregates (D_{max} = 25 mm) ranges between 6.2% and 22.5%. Smaller steel fibres tend to contribute to a higher compressive strength, probably due to their more homogenous distribution inside the concrete matrix.

Fig. 8 shows the tensile strength of the designed UHPFRC after 28 days. The coarse aggregates have a limited negative effect on the tensile strength, from 6.4 MPa to 6.2 MPa, which is similar to that of the compressive strength. After incorporating 2 vol% steel fibres, the tensile strength is improved considerably, with increase ratios between 127% and 170%, due to the bridging effect of steel fibres. However, the effects of reinforcement on tensile strength between different fibre types are not very obvious in the same UHPFRC matrix. The 30 mm medium hook-ended steel fibres show the best reinforcement, followed by the 60 mm long 5D fibres and the 13 mm short straight ones.

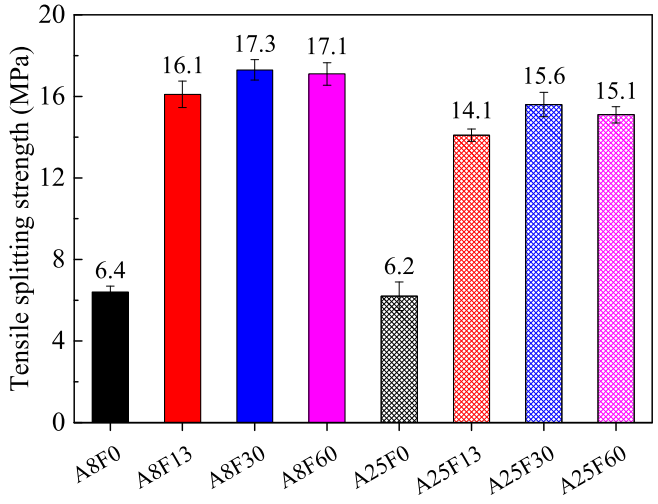

Fig. 8. Tensile splitting strength.

The flexural behaviour of UHPFRC is illustrated by the load-deflection curves or stress-normalized deflection curves in Fig. 9. As illustrated in Fig. 5(b), all the load-deflection curves experience three stages, namely elastic stage from zero point to the first crack point, deflection or strain hardening stage from the first crack point to the peak point, deflection or strain softening stage after peak point. The main key parameters in flexural tests are summarized in Table 4. The slopes (respecting elastic modulus), loads and deflections at the first cracks in the curves without or with different types of steel fibres are very similar, which indicates that the elastic stages are mainly dependent on the UHPFRC matrix instead of the steel fibres. With the inclusion of 2 vol% steel fibres, all the UHPFRC beams exhibit strain hardening behaviours, although it is not obvious in the case of 13 mm short straight fibres. The peak deflection can be greatly enlarged from mixture of A8F0 to A8F60, therefore the ductility of UHPFRC is greatly improved. All the curves of the designed UHPFRC mixtures have long tails during the strain softening stages, revealing the high residual strength and energy absorption ability of the designed UHPFRC.

3.2. Impact properties

3.2.1. Energy dissipation

The impact resistance of UHPFRC beams is represented by the impact number and absorbed energy. Table 5 shows the failure impact number and total absorbed energy calculated based on Eq. (4). The two plain concrete can only suffer from one pendulum impact, which indicates that they are very brittle and not suitable to be used for impact resistant element or structure. Incorporating 2 vol% of 13 mm short straight fibres, the energy dissipation ability of UHPFRC beams can be greatly enhanced, as high as about 5–6 times. The impact resistance is further significantly increased with the inclusion of 2 vol% of 30 mm medium hook-ended or 60 long 5D steel fibres. Thus, the steel fibres are indispensable for UHPFRC subjected to impact loading, due to an increase in fibre pull-out load and strain capacity [5,31]. However, the improvement degrees are not the same for different UHPFRC matrices, which will be discussed in following Section 3.3.3.

To further analyse the impact resistance mechanism and damage propagation, the development of energy absorption during each impact is investigated, as shown in Fig. 10. In this study, the absorbed energy of UHPFRC beam during one impact usually ranges between 35% and 50% as the initial impact energy of hammer (approximately 698 J). For the UHPFRC beam reinforced with steel fibres, the energy absorption development suffers through three stages, firstly dissipating relatively low energy at the initial several impacts, afterwards keeping in a higher and stable level at the following impacts, and then tending to further higher energy absorption and complete failure at the last few impacts. The first stage is more like elastic collisions, transferring more gravitational potential energy into kinetic energy of UHPFRC beam, thus resulting in less energy absorption of material itself. The second stage is mainly due to the fibre pull-out process. The partially damaged UHPFRC beam tends to be 'soft' because of degeneration of stiffness, which contributes to more impact energy transformation into the material deformation energy instead of kinetic energy. The third stage is a failure acceleration stage where damage degree develops faster and faster till the complete breakage from the centre occurs, and more impact energy is absorbed due to large deformation. An example is shown in Fig. 10(a), that the three stages are indicated.

3.2.2. Correlation between impact resistance and flexural properties

Until now there is no standard impact method to measure the impact resistance of UHPFRC, most dynamic or impact testing methods reported in literature are too complex and costly compared to the static properties tests. Thus, it is of great significance if we can predict the

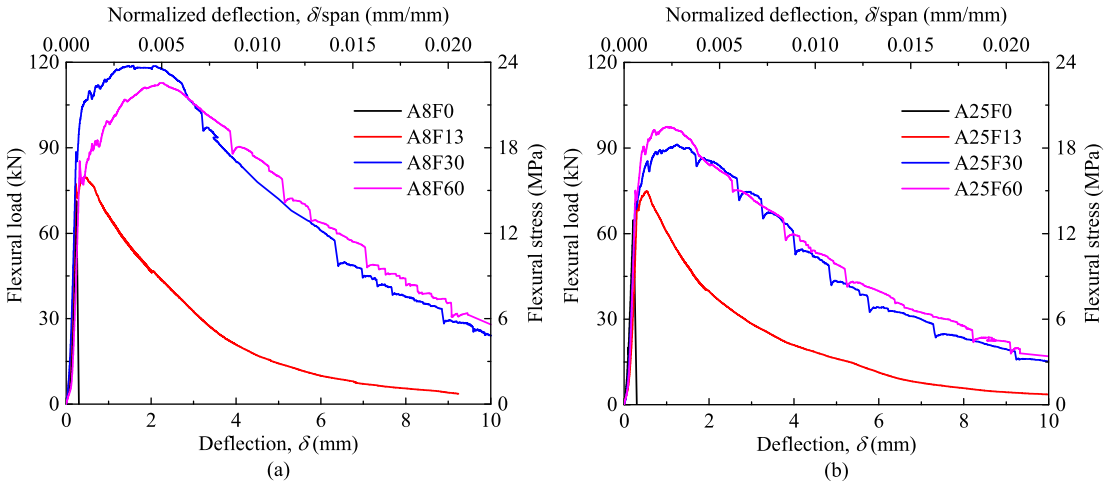

Fig. 9. Flexural load vs. deflection curves.

Table 4
Key parameters of UHPFRC in flexural test (see Fig. 5(b)).

Mix No.	First crack load, P_1 (kN)	First crack stress, σ_1 (MPa)	Peak Load, P_p (kN)	Peak stress, σ_p (MPa)	Toughness, T_f (J)
A8F0	71.2	14.2	71.2	14.2	8.3
A8F13	77.3	15.5	79.6	15.9	235.4
A8F30	88.6	17.7	118.8	23.8	716.1
A8F60	85.4	17.1	112.8	22.6	718.1
A25F0	64.8	13.0	64.8	13.0	7.2
A25F13	70.5	14.1	74.8	15.0	219.3
A25F30	71.3	14.3	91.2	18.2	489.4
A25F60	75.1	15.0	97.4	19.5	516.1

Table 5
Total impact number and energy dissipation.

Mix No.	Failure impact number, N	Energy dissipation, E_{absorb}, (J)
A8F0	1	299
A8F13	6	1833
A8F30	93	27940
A8F60	17	5650
A25F0	1	325
A25F13	5	1561
A25F30	8	2519
A25F60	15	4759

impact resistance of UHPFRC by its static properties. Our previous study has confirmed that the toughness can be used as a good indicator to reflect the impact resistance of UHPFRC [5]. Fig. 11 presents the correlation between impact energy and flexural toughness of the designed UHPFRC beams. A linear analytical model can be introduced to describe this correlation, except for the results of specimen A8F30.

$$E_{absorb} = k \cdot T_f \tag{5}$$

The correlation coefficient k varies from different hammer and beam, such as size, mass, impact velocity, texture etc. The value of k is approximately 7.576 ($R^2 = 0.96$) in this research, which is much larger than the previous study on notched beam with a smaller initial impact energy (346 J) [5]. This enlarged k is probably due to the increased dynamic properties by higher loading rates effect under much stronger impacts (698 J) [43–45].

It should be noted that the result of specimen A8F30 does not fit to this linear model, which shows an impact resistance above the trend line. Because the beam of A8F30 possesses the highest flexural strength as shown in Fig. 9, the stress induced by impacts is possibly below the elastic limits. Thus, the plastic deformation and damage is very limited, resulting in a relatively high residual strength and impact resistance. Fig. 12(a) illustrates the residual strength of composites under different impact energy levels [46], with an obvious threshold value of impact energy. Below the threshold energy, the residual strength remains stable. Thus, there is almost no or only slight damage and the element can withstand many repeated impacts. Fig. 12(b) shows a parabolic relationship between the impact number and impact energy. Under the impact energy higher than the threshold, only a few impact number is observed. When the impact energy value is lower than the threshold, the impact responses behave in elastic state, resulting in a significant increase of impact number [47].

Hence, the impact resistance of UHPFRC beam (absorbed energy or impact number) is greatly dependent on both flexural strength and toughness. It is mainly attributed to the flexural strength when subjected to impacts with the impact energies below the threshold energy. While, flexural toughness determines the impact resistance and shows a linear correlation, if the impact energy is beyond the threshold.

3.3. Discussion

3.3.1. Coarse aggregate effect

When coarse aggregates are introduced into UHPFRC system, the powder consumption tends to decrease, while the interfaces around the coarse aggregates could become the weakest part and be the inherent flaws [48]. Therefore, the effect of coarse aggregates on impact resistance, static properties and economic benefit should be very carefully analysed and discussed. Generally, in this study, the coarse basalt aggregates bring economic benefit by decreasing the powder content from 900 kg/m^3 to 700 kg/m^3, and greatly increasing the binder efficiency. without significantly sacrificing the compressive and tensile strength. The compressive and tensile splitting strengths have limited decrease ratios, no more than 13%, when increasing the D_{max} from 8 mm to 25 mm. The decrease ratios of flexural strength and toughness seem relatively larger, which could be even as high as 23.5% and 31.7%, respectively, compared with mixtures of A8F30 and A25F30. As illustrated in Section 3.2.2, the reduced flexural strength and toughness certainly result in lower energy dissipation ability and impact resistance, namely 14.8%, 91.0% and 15.8% reductions in the presence of different steel fibres. To sum up, considering the benefits brought by coarse aggregates, the negative effect of coarse aggregates on strengths is limited and tolerable. While, the negative effect of aggregate size on toughness and impact resistance is more sensitive than the strengths, which is probably attributed to a faster damage development and lower residual

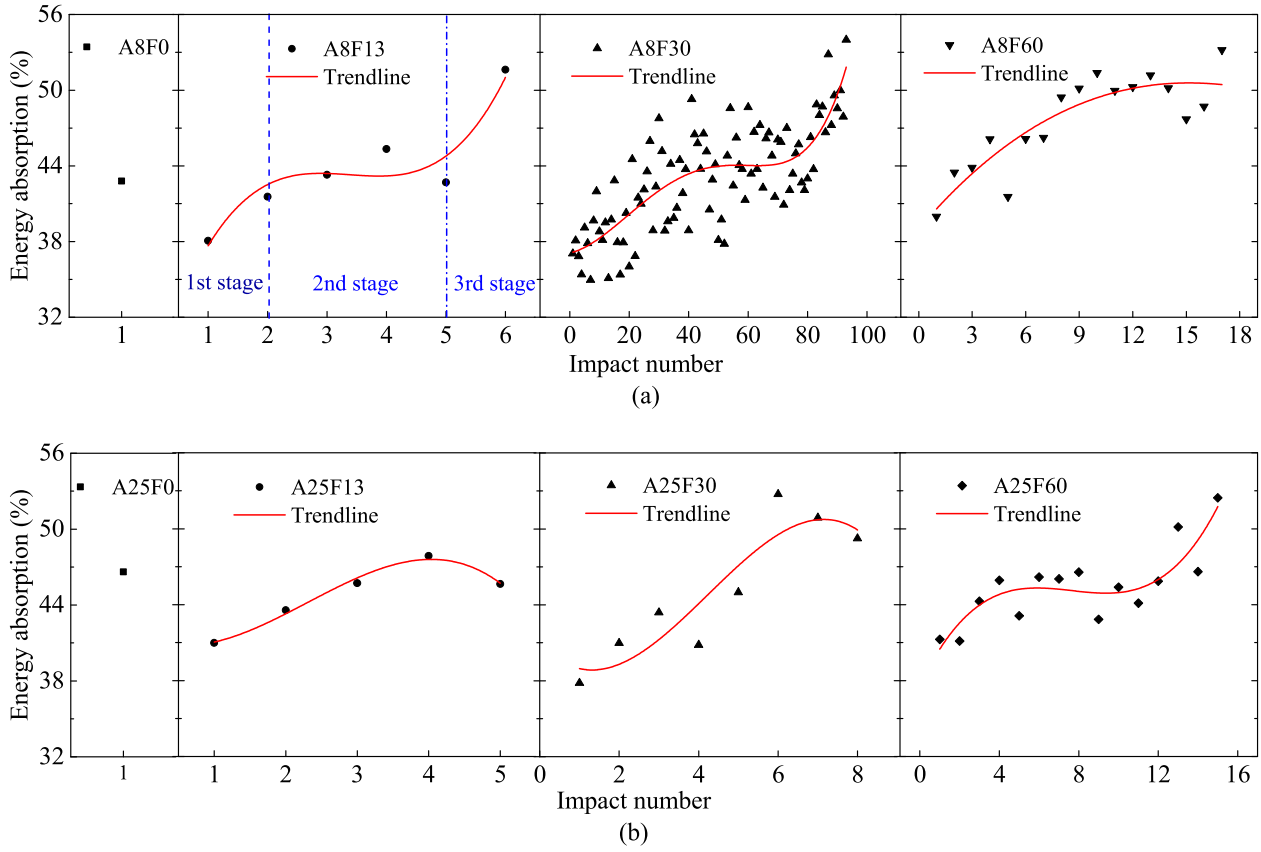

Fig. 10. Development of energy absorption, in (a) an example of 3 impact stages are indicated.

flexural strength for an UHPFRC beam with coarser aggregates.

3.3.2. Steel fibre effect

As mentioned above, the type of steel fibre is another key factor on impact resistance and flexural behaviour of UHPFRC beam. In this section, the effects of three different steel fibres are discussed with a fixed dosage of 2 vol%. Normally, the reinforcement of steel fibres is dependent on the geometric and mechanical characters, utilized dosage and fibre-to-matrix bond. To assess the overall effects of the three different steel fibres on impact resistance and flexural properties, a reinforcing factor η and strain hardening factor φ [49] are introduced,

$$\eta = \frac{X_{UHPFRC}}{X_{matrix}} \tag{6}$$

$$\varphi = \frac{\sigma_p}{\sigma_1} \tag{7}$$

where X_{UHPFRC} and X_{matrix} are the key properties of UHPFRC with and without steel fibres, respectively, such as first crack strength (σ_1), peak strength (σ_p), toughness (T_f) and absorbed impact energy (E_{absorb}).

The reinforcing factors in terms of first crack strength, peak strength, toughness and impact resistance are presented in Table 6. The reinforcing factor in terms of first crack strength ($\eta_{\_\sigma_1}$) changes in a relatively low and narrow range between 1.09 and 1.25, which indicates that the first crack stress is not sensitive to the fibre type effect and is mainly determined by the UHPFRC matrix. The reinforcing factor in terms of peak strength ($\eta_{\_\sigma_p}$) is always clearly larger than that of first crack strength ($\eta_{\_\sigma_1}$) for the same UHPFRC matrix, which means that the steel fibres contribute more to the peak strength rather than the first crack strength. The fibre-to-matrix bonding force is triggered up to the maximum value during the strain hardening stage [50], which results in more efficient reinforcement and thus a larger reinforcing factor $\eta_{\_\sigma_p}$.

The reinforcing factors in terms of impact resistance ($\eta_{\_E_{absorb}}$) and flexural toughness ($\eta_{\_T_f}$) are very considerable, namely several or even dozens of times the flexural strengths. In other words, the energy absorption ability of UHPFRC beam is mainly provided by the "bridge effect" of steel fibres, instead of the UHPFRC matrix. Compared with the reinforcing factors of different steel fibres, the 13 mm short straight fibres show the poorest reinforcement on impact resistance and flexural toughness. The 30 mm medium hook-ended fibres provide the best enhancement for UHPFRC with the finer aggregates (D_{max} = 8 mm), while the 60 mm long 5D fibres are more suitable than the medium ones for the UHPFRC with the coarser basalt aggregates (D_{max} = 25 mm).

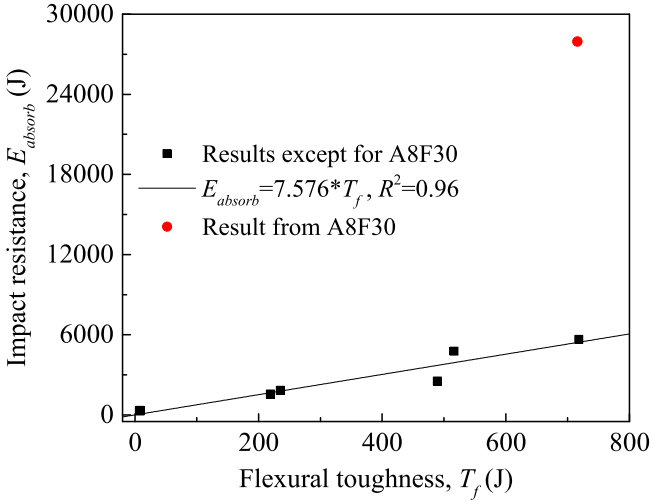

Fig. 11. Correlation between impact energy and flexural toughness.

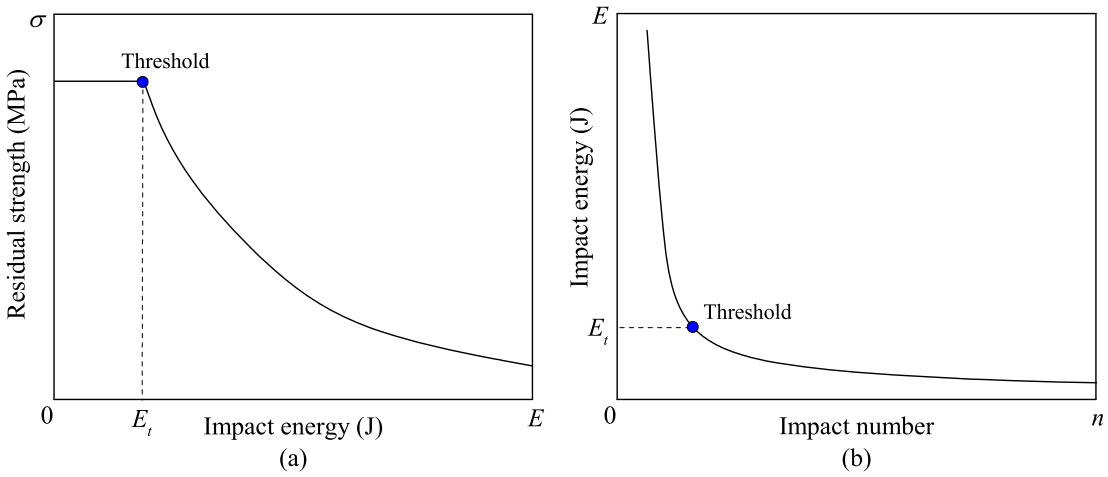

Fig. 12. Effect of impact energy on (a) residual strength and (b) impact number.

The value of strain hardening factor is larger than 1.0 when a strain hardening phenomenon is triggered by the utilized steel fibres, and a larger value means a stronger strain hardening behaviour. The strain hardening factors of UHPFRC beams are shown in Table 6. The strain hardening factors are very close to each other with different UHPFRC matrices incorporating the same type of steel fibres. UHPFRC incorporating the 13 mm short fibres shows a very slight strain hardening behaviour, with a factor φ around 1.04. UHPFRC with the 30 mm medium fibres acquires the strongest strain hardening behaviour incorporating the maximum basalt size of 8 mm (φ = 1.35), followed by the 60 mm long 5D fibres (φ = 1.32). On the one hand, fibres with special shapes of hook or 5D ends can provide a positive anchoring effect compared to the straight fibres. On the other hand, fibres with longer length can enhance the flexural strength and energy absorption capacity by increasing the peak pull-out load and corresponding slip, due to the improvement on effective bonding area of fibres at crack surfaces and fibre orientation [31,51]. When coarser basalt aggregates are included, e.g. maximum size of 25 mm, the long steel fibres show a slightly larger strain hardening factor (1.30) than the medium fibre (1.29).

Table 6
Fibre reinforcing and strain hardening factors for UHPFRC mixtures.

Mix No.	$\eta_{\_\sigma_1}$	$\eta_{\_\sigma_p}$	$\eta_{\_T_f}$	$\eta_{\_E_{absorb}}$	φ
A8F0	1.00	1.00	1.00	1.00	1.00
A8F13	1.09	1.12	28.4	6.13	1.03
A8F30	1.25	1.68	86.3	93.4	1.35
A8F60	1.20	1.59	86.5	18.9	1.32
A25F0	1.00	1.00	1.00	1.00	1.00
A25F13	1.09	1.15	30.5	4.80	1.05
A25F30	1.10	1.40	68.0	7.75	1.29
A25F60	1.15	1.50	71.7	14.6	1.30

3.3.3. *Synergistic effect between aggregate and fibre*

As illustrated in Table 5, the improvement degrees on impact resistance by different steel fibres are not the same for different UHPFRC matrices. A synergistic effect between aggregate and fibre is observed, namely UHPFRC with the smaller basalt aggregates is preferred to the 30 mm medium hook-ended fibres to achieve the best impact resistant mixture (A8F30), while the coarser basalt aggregates need much longer steel fibres (60 mm long 5D) to acquire enough reinforcement (A25F60). Because the impact resistance is linked to the static flexural properties, as demonstrated in Section 3.2.2, a similar synergistic effect can also be obtained in flexural properties. The order of reinforcement on flexural properties is as follows: 30 mm medium hook-ended fibre >60 mm long 5D fibre >13 mm short straight fibre for UHPFRC with the D_{max} of 8 mm, while 60 mm long 5D fibre >30 mm medium hook-ended fibre >13 mm

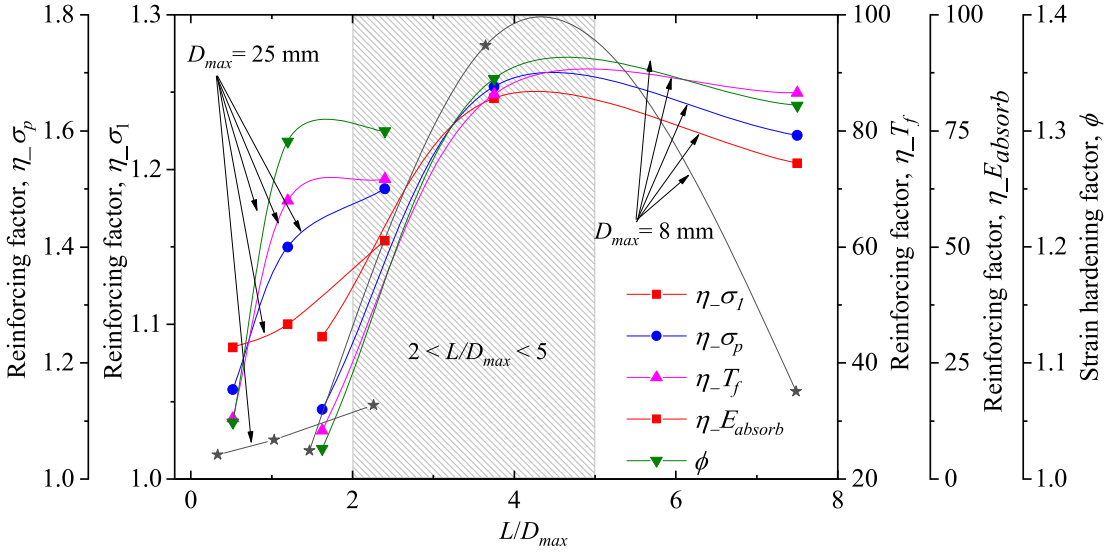

Fig. 13. Correlation between L/D_{max} and fibre utilization.

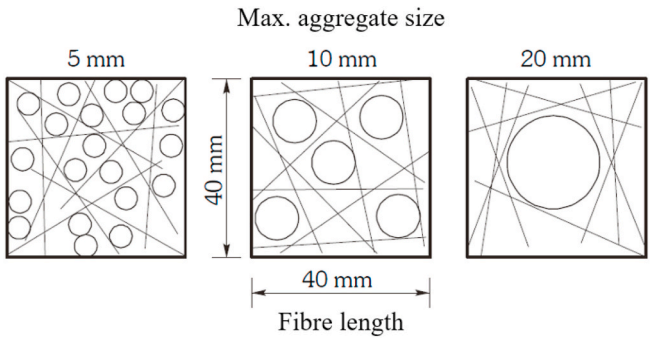

Fig. 14. Interaction between aggregates and steel fibres on granular skeleton [32].

short straight fibre for UHPFRC with the D_{max} of 25 mm.

Due to the inherent correlation between impact resistance and flexural properties, the relative size effect (ratio of fibre length to maximum aggregate size, L/D_{max}) on the both impact and static parameters ($\eta_{\_\sigma_1}$, $\eta_{\_\sigma_p}$, $\eta_{\_T_f}$, $\eta_{\_E_{absorb}}$ and φ) are used to reveal the interaction between aggregates and steel fibres, as illustrated in Fig. 13. The lowest utilization efficiency is obtained with the short steel fibres, which is in line with the results observed in the UHPFRC incorporating coarse aggregates [16]. Firstly, the straight fibres have weaker bond compared to other fibres with anchoring effect at ends. Additionally, the short fibres cannot completely overlay aggregates with a large size, thus providing a limited fibre-bridging interlock stress. Furthermore, if the size of coarse aggregate is too large compared to the fibre length, the fibre distribution in matrix can be significantly disturbed, as shown in Fig. 14. The non-random orientation of steel fibres adversely affects the reinforcement efficiency and decreases the compactness.

Preferential synergistic effects are observed between aggregates with the maximum size of 8 mm and 30 mm medium hook-ended fibres (A8F30), aggregates with the maximum size of 25 mm and 60 mm long 5D fibres (A25F60), considering all fibre utilization factors ($\eta_{\_\sigma_1}$, $\eta_{\_\sigma_p}$, $\eta_{\_T_f}$, $\eta_{\_E_{absorb}}$ and φ) in Fig. 13. Thus, a longer fibre is not always better, and an appropriate length of steel fibre is needed to match the size of coarse aggregate. On the one hand, longer fibres are beneficial to overlay coarse aggregates, enhance the interlock between fibres and coarse aggregates and then improve the flexural performance [31,48]. On the other hand, limiting the particle size to half the fibre length is recommended from the workability point of view [32], which can also decrease the probability of the 'fibre balling' phenomenon. Han et al. indicated that the rational range of the ratio of steel fibre length to coarse aggregate maximum size for steel fibre reinforced concrete is 1.25–3 by considering the reinforcements on splitting tensile strength and flexural properties [33]. Rui et al. summarized that the fibre length is mostly about 2–4 times of the maximum aggregate size in normal concrete, at least not shorter than the aggregate size [52]. Based on the acquired results, the length of steel fibre (L) is recommended to be between 2 and 5 times the maximum size of aggregate (D_{max}) for UHPFRC systems, as illustrated in Fig. 13. In the case of a smaller D_{max}, the L/D_{max} tends to a larger value.

4. Conclusions

This paper studies the synergistic effect between steel fibres and coarse aggregates on impact resistance of UHPFRC applying a pendulum impact test setup. The aggregate size effect, steel fibre type effect, and their interaction are analysed. Moreover, correlations between impact resistance and static mechanical properties are established. The key conclusions can be summarized:

- Coarse basalt aggregates up to 25 mm can be successfully introduced into UHPFRC with a significantly lowered cement consumption, designed by using a particle packing model, with limited influence on compressive and tensile splitting strengths. However, the negative influence of basalt size effect is more obvious on impact resistance and flexural toughness. The maximum size of coarse aggregate is suggested to be no more than 25 mm.
- The 13 mm short straight steel fibres show a good reinforcement on compressive strength due to the more homogenous distribution in UHPFRC matrix. While, the 30 mm medium hook-ended or 60 mm long 5D fibres are more efficient in reinforcing tensile, flexural and impact properties.
- Based on the analysis of fibre reinforcing factors, the impact resistance and flexural toughness are more sensitive to the steel fibres, followed by the flexural peak strength, while the first crack strength is mainly controlled by the UHPFRC matrix.
- The deflection or strain hardening behaviour can be acquired by utilizing 2 vol% of 30 mm medium hook-ended or 60 mm long 5D steel fibres, while the 13 mm short straight fibres only trigger a very limited strain hardening behaviour.
- A preferential synergistic effect is observed between the coarser aggregates and the longer steel fibres. The length of steel fibre is suggested between 2 and 5 times as the maximum size of aggregate. The order of reinforcement on impact and flexural properties is: 30 mm hook-ended fibre >60 mm 5D fibre >13 straight fibre for UHPFRC with the D_{max} of 8 mm, while 60 mm 5D fibre >30 mm hook-ended fibre >13 straight fibre for UHPFRC with a D_{max} of 25 mm.
- The flexural strength determines the threshold of impact energy, and it is the main factor to control the impact resistance of UHPFRC beam subjected to impact loadings below the threshold. While the flexural toughness shows a linear relationship on impact resistance of UHPFRC beam when the impact energy exceeds the threshold.

Data availability

The raw/processed data required to reproduce these findings cannot be shared at this time as the data also forms part of an ongoing study.

Declaration of competing interest

The authors declare that they have no known competing financial interests or personal relationships that could have appeared to influence the work reported in this paper.

Acknowledgements

This research was funded by China Scholarship Council and Eindhoven University of Technology. Authors thank Mr. Ad. Verhagen, Mr. Gang Liu, Mr. YuXuan Chen and Mr. Tao Liu to help the experiments. The authors are also grateful to ENCI, Bekaert and Sika for supplying the cement, steel fibres and superplasticizer, respectively.

References

[1] D. Wang, C. Shi, Z. Wu, J. Xiao, Z. Huang, Z. Fang, A review on ultra high performance concrete: Part II. Hydration, microstructure and properties, Construct. Build. Mater. 96 (2015) 368–377.
[2] Y. Wang, J.Y.R. Liew, S.C. Lee, Theoretical models for axially restrained steel-concrete-steel sandwich panels under blast loading, Int. J. Impact Eng. 76 (2015) 221–231.
[3] S.-T. Kang, Y. Lee, Y.-D. Park, J.-K. Kim, Tensile fracture properties of an ultra high performance fiber reinforced concrete (UHPFRC) with steel fiber, Compos. Struct. 92 (2010) 61–71.
[4] R. Yu, P. Spiesz, H.J.H. Brouwers, Static properties and impact resistance of a green ultra-high performance hybrid fibre reinforced concrete (UHPHFRC): experiments and modeling, Construct. Build. Mater. 68 (2014) 158–171.
[5] P.P. Li, Q.L. Yu, Responses and post-impact properties of ultra-high performance fibre reinforced concrete under pendulum impact, Compos. Struct. 208 (2019) 806–815.

[6] C. Shi, Z. Wu, J. Xiao, D. Wang, Z. Huang, Z. Fang, A review on ultra high performance concrete: Part I. Raw materials and mixture design, Construct. Build. Mater. 96 (2015) 368–377.
[7] P. Richard, M. Cheyrezy, Composition of reactive powder concretes, Cement Concr. Res. 25 (1995) 1501–1511.
[8] P.P. Li, Y.Y.Y. Cao, H.J.H. Brouwers, W. Chen, Q.L. Yu, Development and properties evaluation of sustainable ultra-high performance pastes with quaternary blends, J. Clean. Prod. 240 (2019), 118124.
[9] R. Yu, L. van Beers, P. Spiesz, H.J.H. Brouwers, Impact resistance of a sustainable ultra-high performance fibre reinforced concrete (UHPFRC) under pendulum impact loadings, Construct. Build. Mater. 107 (2016) 203–215.
[10] P.P. Li, H.J.H. Brouwers, Q. Yu, Influence of key design parameters of ultra-high performance fibre reinforced concrete on in-service bullet resistance, Int. J. Impact Eng. 136 (2020), 103434.
[11] D.Y. Yoo, N. Banthia, S.T. Kang, Y.S. Yoon, Effect of fiber orientation on the rate-dependent flexural behavior of ultra-high-performance fiber-reinforced concrete, Compos. Struct. 157 (2016) 62–70.
[12] H.-O. Shin, K.-H. Min, D. Mitchell, Confinement of ultra-high-performance fiber reinforced concrete columns, Compos. Struct. 176 (2017) 124–142.
[13] K. Wille, C. Boisvert-Cotulio, Material efficiency in the design of ultra-high performance concrete, Construct. Build. Mater. 86 (2015) 33–43.
[14] R. Zhong, K. Wille, R. Viegas, Material efficiency in the design of UHPC paste from a life cycle point of view, Construct. Build. Mater. 160 (2018) 505–513.
[15] R. Yu, P. Spiesz, H.J.H. Brouwers, Mix design and properties assessment of ultra-high performance fibre reinforced concrete (UHPFRC), Cement Concr. Res. 56 (2014) 29–39.
[16] P.P. Li, Q.L. Yu, H.J.H. Brouwers, Effect of coarse basalt aggregates on the properties of Ultra-high Performance Concrete (UHPC), Construct. Build. Mater. 170 (2018) 649–659.
[17] T. Dittmer, H. Beushausen, The effect of coarse aggregate content and size on the age at cracking of bonded concrete overlays subjected to restrained deformation, Construct. Build. Mater. 69 (2014) 73–82.
[18] Y. Peng, H. Wu, Q. Fang, J.Z. Liu, Z.M. Gong, Impact resistance of basalt aggregated UHP-SFRC/fabric composite panel against small caliber arm, Int. J. Impact Eng. 88 (2016) 201–213.
[19] S. Collepardi, L. Coppola, R. Troli, M. Collepardi, Mechanical properties of modified reactive powder concrete, ACI Spec. Publ. 173 (1997) 1–22.
[20] K. Wille, A.E. Naman, G.J. Parra-Montesinos, Ultra-high performance concrete with compressive strength exceeding 150 MPa (22ksi) : a simpler way, ACI Mater. J. 108 (2011) 46–53.
[21] C. Jiang, Y.F. Wu, J.F. Jiang, Effect of aggregate size on stress-strain behavior of concrete confined by fiber composites, Compos. Struct. 168 (2017) 851–862.
[22] L. Soufeiani, S.N. Raman, MZ Bin Jumaat, U.J. Alengaram, G. Ghadyani, P. Mendis, Influences of the volume fraction and shape of steel fibers on fiber-reinforced concrete subjected to dynamic loading – a review, Eng. Struct. 124 (2016) 405–417.
[23] Y.Y.Y. Cao, P.P. Li, H.J.H. Brouwers, M. Sluijsmans, Q.L. Yu, Enhancing flexural performance of ultra-high performance concrete by an optimized layered-structure concept, Compos. B Eng. 171 (2019) 154–165.
[24] D.-Y. Yoo, J.-H. Lee, Y.-S. Yoon, Effect of fiber content on mechanical and fracture properties of ultra high performance fiber reinforced cementitious composites, Compos. Struct. 106 (2013) 742–753.
[25] J.H. Lee, Influence of concrete strength combined with fiber content in the residual flexural strengths of fiber reinforced concrete, Compos. Struct. 168 (2017) 216–225.
[26] H. Kim, G. Kim, J. Nam, J. Kim, S. Han, S. Lee, Static mechanical properties and impact resistance of amorphous metallic fiber-reinforced concrete, Compos. Struct. 134 (2015) 831–844.
[27] Z. Wu, C. Shi, W. He, L. Wu, Effects of steel fiber content and shape on mechanical properties of ultra high performance concrete, Construct. Build. Mater. 103 (2016) 8–14.
[28] R. Yu, Q. Song, X. Wang, Z. Zhang, Z. Shui, H.J.H. Brouwers, Sustainable development of Ultra-High Performance Fibre Reinforced Concrete (UHPFRC): towards to an optimized concrete matrix and efficient fibre application, J. Clean. Prod. 162 (2017) 220–233.
[29] Z. Wu, C. Shi, W. He, D. Wang, Static and dynamic compressive properties of ultra-high performance concrete (UHPC) with hybrid steel fiber reinforcements, Cement Concr. Compos. 79 (2017) 148–157.
[30] D.J. Kim, S.H. Park, G.S. Ryu, K.T. Koh, Comparative flexural behavior of hybrid ultra high performance fiber reinforced concrete with different macro fibers, Construct. Build. Mater. 25 (2011) 4144–4155.
[31] D.Y. Yoo, S.T. Kang, Y.S. Yoon, Enhancing the flexural performance of ultra-high-performance concrete using long steel fibers, Compos. Struct. 147 (2016) 220–230.
[32] C.D. Johnston, Proportioning, Mixing and Placement of Fibre-Reinforced Cements and Concretes, Production Methods and Workability of Concrete, E & FN Spon, London, 1996, pp. 155–180.
[33] J. Han, M. Zhao, J. Chen, X. Lan, Effects of steel fiber length and coarse aggregate maximum size on mechanical properties of steel fiber reinforced concrete, Construct. Build. Mater. 209 (2019) 577–591.
[34] R. Yu, Development of Sustainable Protective Ultra-high Performance Fibre Reinforced Concrete (UHPFRC). PhD Thesis. Eindhoven, the Netherland, Eindhoven Universtiy of Technology, 2015.
[35] P.P. Li, Q.L. Yu, H.J.H. Brouwers, Effect of PCE-type superplasticizer on early-age behaviour of ultra-high performance concrete (UHPC), Construct. Build. Mater. 153 (2017) 740–750.
[36] Q.S. Banyhussan, G. Yıldırım, E. Bayraktar, S. Demirhan, M. Şahmaran, Deflection-hardening hybrid fiber reinforced concrete: the effect of aggregate content, Construct. Build. Mater. 125 (2016) 41–52.
[37] H.J.H. Brouwers, H.J. Radix, Self-compacting concrete: theoretical and experimental study, Cement Concr. Res. 35 (2005) 2116–2136.
[38] H.J.H. Brouwers, Particle-size distribution and packing fraction of geometric random packings, Phys. Rev. E 74 (2006), 031309.
[39] Q.L. Yu, P. Spiesz, H.J.H. Brouwers, Development of cement-based lightweight composites - Part 1: mix design methodology and hardened properties, Cement Concr. Compos. 44 (2013) 17–29.
[40] EN 12390-6, Testing Hardened Concrete - Part 6: Tensile Splitting Strength of Test Specimens, Br Stand Institution-BSI CEN Eur Comm Stand, 2009.
[41] EN 12390-3, Testing Hardened Concrete - Part 3: Compressive Strength of Test Specimens, Br Stand Institution-BSI CEN Eur Comm Stand, 2009.
[42] EN 12390-5, Testing Hardened Concrete - Part 5: Flexural Strength of Test Specimens, Br Stand Institution-BSI CEN Eur Comm Stand, 2009.
[43] Y.Y.Y. Cao, Q.L. Yu, H.J.H. Brouwers, W. Chen, Predicting the rate effects on hooked-end fiber pullout performance from Ultra-High Performance Concrete (UHPC), Cement Concr. Res. 120 (2019) 164–175.
[44] Y.S. Tai, S. El-Tawil, T.H. Chung, Performance of deformed steel fibers embedded in ultra-high performance concrete subjected to various pullout rates, Cement Concr. Res. 89 (2016) 1–13.
[45] A. Caverzan, E. Cadoni, M. Di Prisco, Tensile behaviour of high performance fibre-reinforced cementitious composites at high strain rates, Int. J. Impact Eng. 45 (2012) 28–38.
[46] S. Mouhoubi, K. Azouaoui, Residual Properties of Composites Based on Glass Fiber Cloth of Satin 8 Weaving under Impact-Fatigue Loading, 22ème Congrès Français de Mécanique, Lyon, 2015.
[47] A. Akatay, M.Ö. Bora, O. Çoban, S. Fidan, V. Tuna, The influence of low velocity repeated impacts on residual compressive properties of honeycomb sandwich structures, Compos. Struct. 125 (2015) 425–433.
[48] J. Liu, F. Han, G. Cui, Q. Zhang, J. Lv, L. Zhang, et al., Combined effect of coarse aggregate and fiber on tensile behavior of ultra-high performance concrete, Construct. Build. Mater. 121 (2016) 310–318.
[49] S.H. Park, D.J. Kim, G.S. Ryu, K.T. Koh, Tensile behavior of ultra high performance hybrid fiber reinforced concrete, Cement Concr. Compos. 34 (2012) 172–184.
[50] Y.Y.Y. Cao, Q.L. Yu, Effect of inclination angle on hooked end steel fiber pullout behavior in ultra-high performance concrete, Compos. Struct. 201 (2018) 151–160.
[51] D.Y. Yoo, S.T. Kang, Y.S. Yoon, Effect of fiber length and placement method on flexural behavior, tension-softening curve, and fiber distribution characteristics of UHPFRC, Construct. Build. Mater. 64 (2014) 67–81.
[52] S. Grünewald, Performance-based Design of Self-Compacting Fibre Reinforced Concrete, Delft University of Technology, 2004.